EXPERIMENTAL PARAMETRIC INVESTIGATION OF AERODYNAMIC AND AEROACOUSTIC PERFORMANCE OF SMALL-SIZE COMMERCIAL UAV PROPELLERS: COMPARISON OF CONVENTIONAL AND TOROIDAL DESIGNS

Luana G. Stoica[1], Alessandro Di Marco[1], Giorgia Capobianchi[1], Simone Mattiangeli[1]
[1] *DICITA, University of Roma Tre, Italy*

Abstract

The spreading use of small UAVs makes their noise emissions a compelling issue for their social acceptance and public health impact. In this context, understanding the mechanisms of noise generation and identifying effective strategies for noise mitigation could favour a sustainable integration of UAVs into populated environments. To this aim, a parametric experimental study was conducted on a set of commercial off-the-shelf 5-inch UAV propellers. The study systematically examined the influence of design parameters such as blade pitch, number of blades, and blade geometry on the acoustic emission across different rotational regimes. The propellers were tested in single configuration as well as installed on a quadcopter. A comparison with recently introduced toroidal propellers was made to evaluate whether this unconventional geometry provides tangible benefits in terms of noise reduction without compromising thrust generation. Simultaneous measurements using a hot wire anemometer and microphones located in the nearfield and the farfield with respect to the source enabled the correlation of acoustic emissions with the underlying flow structures and unsteady phenomena responsible for sound generation. The results provide insight into the aeroacoustic performance of these systems, offering guidance for the development of quieter UAVs.

Keywords: *UAV, propellers, experimental aeroacoustics, toroidal propellers*

1. Introduction

UAV propeller noise research has recently shifted from simply identifying dominant sources to redesigning blade geometry so that vortices, trailing-edge turbulence, and blade-passing tones are weakened at the source. Across the recent literature, the most consistent advances come from passive geometric changes, such as twist, sweep, serrations, tip modifications, enlarged blade area, and looped or toroidal closures, that target tip-vortex strength and trailing-edge unsteadiness while trying to preserve thrust and efficiency. Recent studies suggest that optimized conventional blades can often deliver modest but reliable reductions of about 3–8 dB.

Twisted blades reduced OASPL by up to 4.3 dB while improving figure of merit by 9.3% [1]. Enlarged blade-area designs achieved 8.1 dBA reduction in flight while also cutting tonal and high-frequency broadband noise [2]. Bio-inspired forward–backward swept tips reduced OASPL by up to 4 dB and broadband noise by about 7 dB by stabilizing the flow over the outboard blade region [3].

Serrated and biomimetic edges remain one of the most active areas. Leading-edge serrations reduced noise by up to 3 dB, with moderate serration size giving the best noise–performance trade-off [4]. Coupled leading- and trailing-edge serrations achieved 3.1 dB laboratory reductions and 2.6–3.8 dB reductions on a hovering quadrotor while also improving thrust efficiency by 7.9% [5].

Toroidal and loop-type propellers are the most visible unconventional advance because they close or partially close the blade tip, directly targeting tip leakage and vortex roll-up. Experimental and numerical studies generally report quieter operation, including radial and axial reductions of 5.2 and 19.6 dB(A) at matched thrust in one toroidal design, 2–3 dB reductions in a toroidal biloop prototype, and about 15 dB reduction in a three-blade loopprop's blade-passing tone with comparable aerodynamic performance [6] [7] [8]. However, toroidal results are not uniformly superior: a multi-objective comparison found toroidal rotors quieter

Corresponding author: *luana.stoica@uniroma3.it.*

than conventional two-blade rotors but less efficient, and noisier than optimized four-blade rotors [9]. That caveat matters because matched-performance comparisons show that some noise gains attributed to exotic geometries can disappear if rotational speed, blade count, or thrust are not controlled carefully [10] [9]. The present study experimentally assesses the aerodynamic and aeroacoustic performance of conventional and unconventional 5-inch UAV propellers under hover and forward-flight conditions. Simultaneous hot-wire and acoustic measurements are used to investigate the relationship between wake development and noise generation, with particular emphasis on the comparison between conventional and toroidal geometries. The experimental setup is described in Section 2, the results are presented and discussed in Section 3, and the main conclusions are summarized in Section 4.

2. Experimental Set-up

Experiments were carried out in the Fluid Dynamics Laboratory of University of Roma Tre.

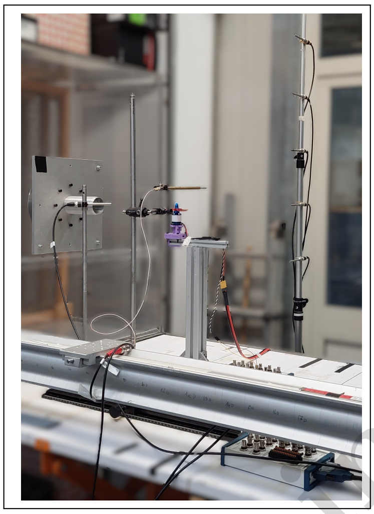

Figure 1: Picture of the experimental set-up.

Nine commercially available propellers with varying diameters, pitch angles, and blade counts Z were tested (see Table 1 and Fig. 2). Among them, as unconventional geometry features, the Dalprop 5145 featured a toroidal blade geometry, while the Gemfan 5152S incorporated winglets at the blade tips. Two operating conditions were investigated: (i) a quiescent environment, representing hover flight, and (ii) a uniform inflow generated by a subsonic jet at 20 m/s, representative of forward-flight conditions. All propellers were evaluated at a constant rotational speed of 12000 rpm.
Each propeller was mounted on a support structure positioned in front of the subsonic jet nozzle, aligned with its centreline and located at a distance equal to six nozzle diameters. The propellers were driven by a Sunnysky X2216 V3 brushless motor (KV 1250) and controlled using a Hobbywing XRotor-40A electronic speed controller.

Table 1: Specifications of the propellers tested.

Propeller	Diameter ["]	Pitch ["]	Z
T-motor T5143S	5.1	4.3	3
Gemfan 51433	5.1	4.33	3
Gemfan 51466	5.1	4.66	3
Gemfan 5152S	5.1	5.2	3
HQProp 5.5x3.5	5.5	3.5	3
APC 5x5E	5	5	2
APC 5x4.75	5	4.75	2
APC 5x5.5	5	5.5	2
DalProp 5145	5.1	4.5	2

Figure 2: Propellers tested.

Acoustic measurements were performed using six Microtech Gefell M360 electret microphones, comprising one near-field microphone and five far-field microphones. The near-field microphone was positioned at a distance of $1D$ from the propeller tip, while the far-field microphones were arranged along a line parallel to the propeller axis at a distance of $5.8D$, with a spacing of $1.65D$ between adjacent microphones. Here, D denotes the reference propeller diameter of 5 inches. The propeller was installed in a pusher configuration, such that the microphones above the propeller plane were able to capture the acoustic emissions of the wake flow. The microphone signals were acquired using a National Instruments PXI-6143 data acquisition system housed in a PXIe-1065 chassis and interfaced through a BNC-2110 connector block. Measurements were acquired over a duration of 10 s at a sampling rate of 100 kHz.
Flow velocity measurements were obtained with an AA Lab Systems AN-1003 hot-wire anemometer equipped with a DANTEC Dynamics Type 55 probe. The probe was located 2.5 inches downstream of the propeller plane and traversed across half of the propeller diameter. A photograph of the experimental setup is provided in Fig. 1.

3. Results

3.1. Velocity measurements

In the following, the mean effective velocity (Fig. 3) measured by the anemometer is shown for all propellers tested, together with the relative turbulence level - RTL (Fig. 4). The x axis is normalized by the radius R of each propeller, with the origin at the propeller hub.

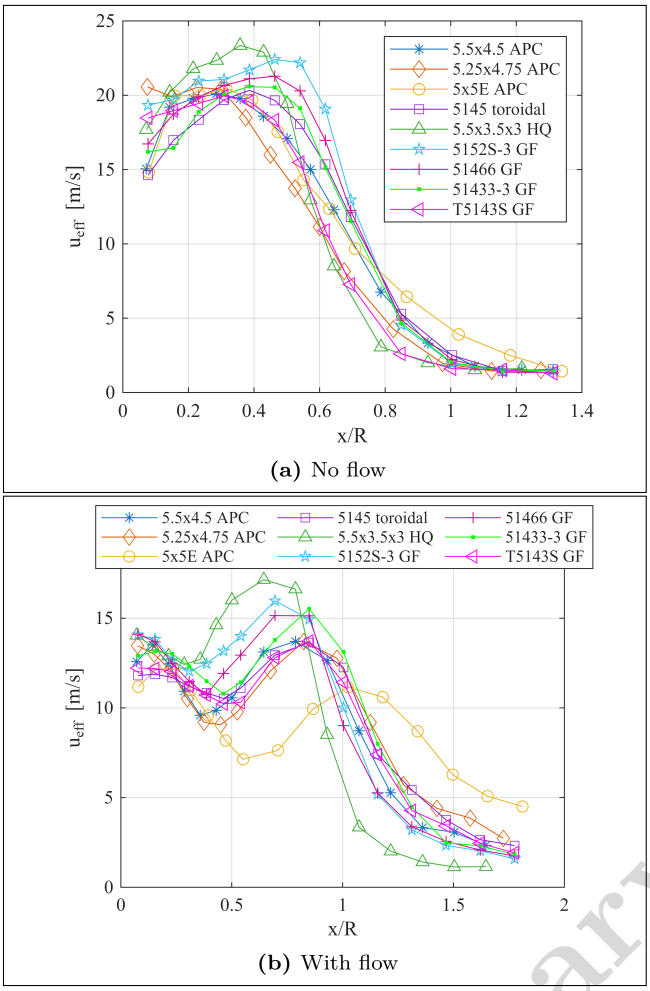

(a) No flow

(b) With flow

Figure 3: Mean effective velocity at different radial stations along the blade.

When the propeller rotates under hover conditions, the wake velocity exhibits a local minimum at the hub, reaches a maximum between $0.3 - 0.6R$, and then gradually converges to approximately 1.5 m/s outside the propeller disk. This value is attained at about 1.1R for all propellers except the APC 5x5E, for which convergence occurs farther downstream, at approximately $1.3R$. The relative turbulence intensity shows a minimum around $0.3 - 0.4R$ and a maximum whose location depends on the propeller geometry, typically occurring between $0.8 - 0.9R$. Under inflow conditions, the wake is displaced in the direction of the incoming flow. The magnitude of this displacement varies among the propellers considered. A comparable shift is also observed in the relative turbulence intensity distribution.

3.2. Acoustic measurements

In this Section, the acoustic performance of the propellers tested are examined.

Fig. 5 reports the OASPL measured along the propeller axis for the different propeller geometries. The microphone position (x_m) is normalised with the diameter of each propeller.

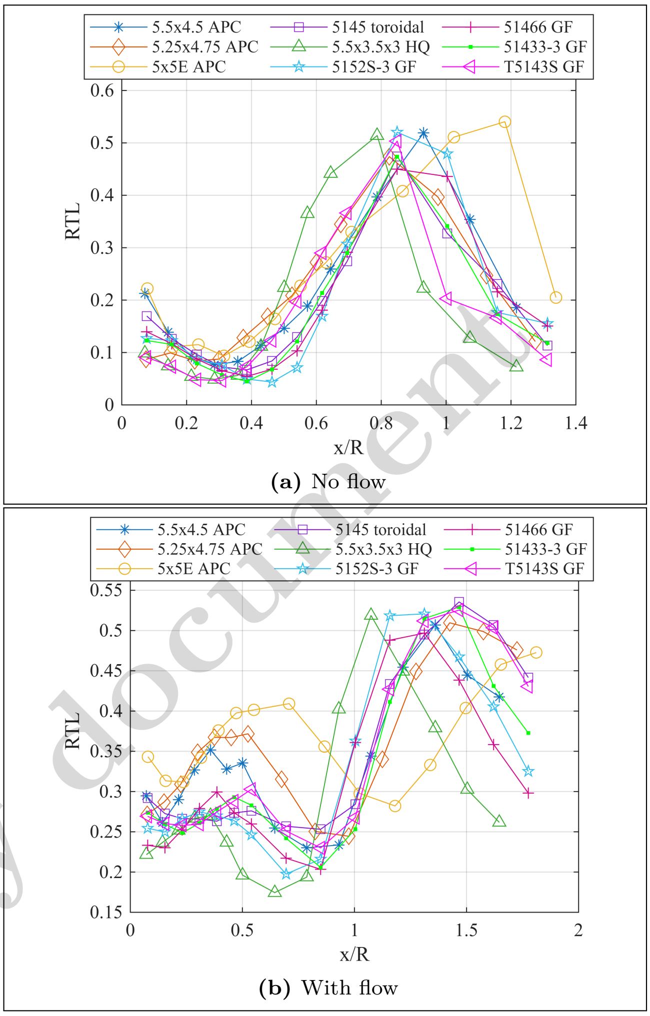

(a) No flow

(b) With flow

Figure 4: Relative turbulence level at different radial stations along the blade.

Negative values of x_m/D correspond to microphones located upstream of the rotor plane, while positive values correspond to positions in the wake. Solid lines represent hover conditions and dashed lines represent forward-flight conditions with an incoming flow velocity of 20 m/s.

The minimum OASPL is generally observed at the rotor plane ($x_m/D = 0$), followed by a local maximum in the near wake around $x_m \approx 1.5$. Further downstream, the acoustic levels gradually decrease.

Under hover conditions (no incoming flow), the two-bladed propellers exhibit higher noise levels than the three-bladed configurations. The toroidal geometry (Dalprop 5145) shows an intermediate OASPL value, lying between those of the two-bladed and three-bladed propellers. This result highlights the effectiveness of the toroidal geometry in mitigating noise generation when compared with conventional two-bladed designs. Comparable acoustic levels are observed for the winglet-equipped propeller (GF 5152S-3). Among the quietest configurations are the propeller with the largest diameter (HQ 5.5×3.5×3) and those characterized by the highest pitch angles (GF 51466 and GF 5152S).

The introduction of a 20 m/s crossflow significantly alters the acoustic field. For all propellers, the measured OASPL increases by approximately 4-8 dB over the entire measurement region. This increase is particularly evident downstream of the rotor, where the wake interacts with the incoming flow and generates additional loading fluctuations and turbulent structures. In contrast to the hover condition, acoustic levels remain high far into the wake, indicating that the principal noise-generating mechanisms become more strongly coupled with the displaced wake flow. In this condition, the toroidal propeller becomes the quietest configuration, whereas the conventional two-bladed propellers remain the noisiest, although with a different relative ranking from that observed under hover conditions. This behaviour suggests a reduced generation, or a faster decay, of coherent wake structures contributing to acoustic radiation for the toroidal geometry. The result is consistent with the CPSD analysis in Section 3.3, which shows a weaker velocity-pressure coupling for the toroidal geometry in the wake region.

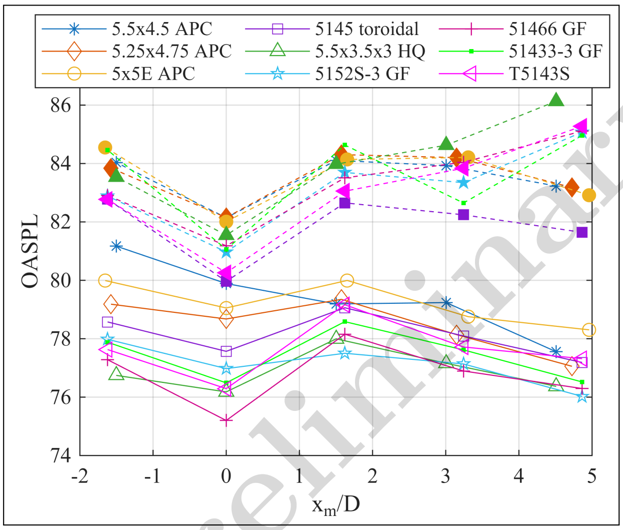

Figure 5: OASPL measured with (dashed line) and without flow (solid lines) for the different propellers tested.

The acoustic spectra measured for the different propellers in hover are reported in Fig. 6 a), together with the background noise (BN). The microphone considered is located at a height of $\approx 5D$ from the propeller plane, resulting in $\approx 7.6D$ (with $D = 5in.$) distance from the propeller hub and represents the furthest observer considered in the study. The sound pressure spectral level (L_p) was computed using the Welch method, with a Hamming window of 65536 length and 50% overlap. Significant variations are observed in the broadband component of the spectra.

The APC 5×5E shows the greatest acoustic contribution at low and intermediate frequencies. Conversely, the T5143S displays among the highest spectral levels in the high-frequency range. The GF 5152S-3, characterized by the highest pitch angle of all the propellers tested, exhibits the lowest high-frequency noise levels. The spectra obtained in the presence of incoming flow are shown in Fig. 6 b). In this case, the acoustic spectra exhibit a much higher degree of similarity.

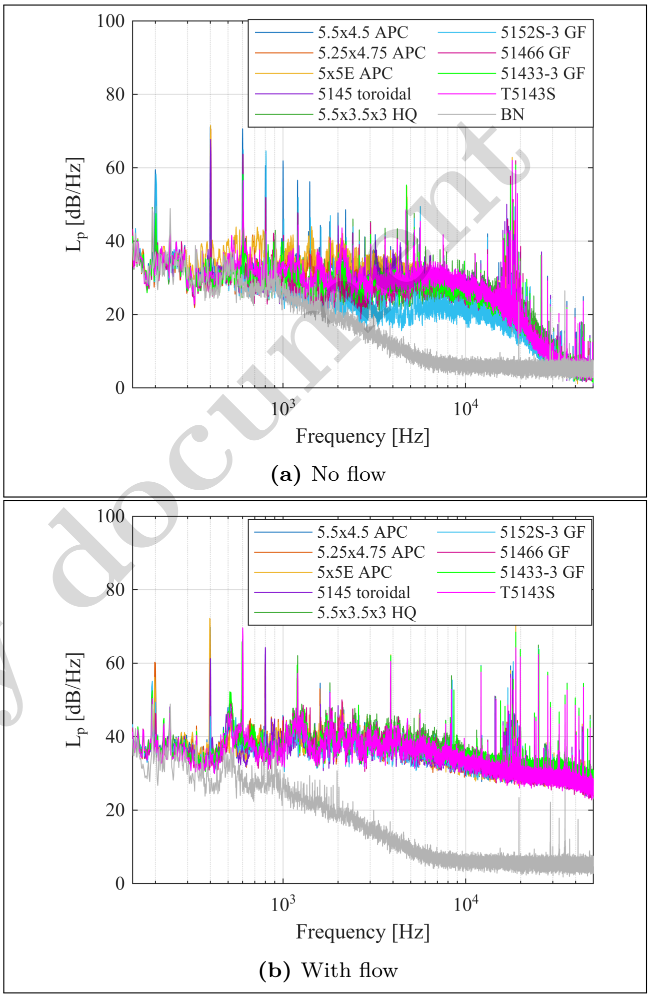

(a) No flow

(b) With flow

Figure 6: Farfield acoustic spectra at 7.6D for the different propellers tested.

3.3. Pressure-velocity correlation

In this section, the correlation between local flow velocity along the blade span and the acoustic pressure signal acquired by the furthest far-field microphone is analysed.

Fig. 7 a) presents the cross-spectral density (CPSD) between the local velocity fluctuations measured at different radial positions and the far-field acoustic pressure signal for the 5145 toroidal propeller. Distinct tonal components are observed at the blade passing frequency (BPF) and its harmonics, indicating a significant correlation between the aerodynamic fluctuations in the rotor flow and the radiated acoustic field.

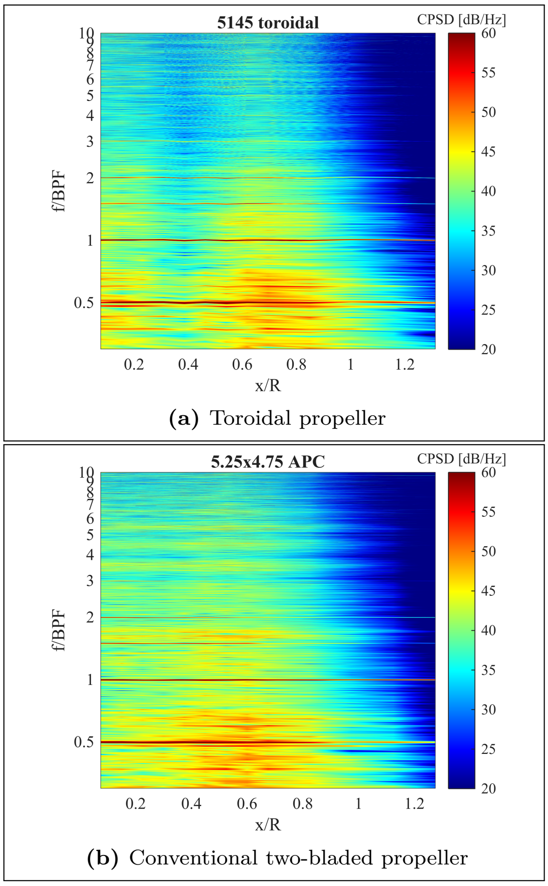

(a) Toroidal propeller

(b) Conventional two-bladed propeller

Figure 7: CPSD between the local velocity fluctuations measured at different radial positions and the far-field acoustic pressure signal from the furthest observer position. No flow (hover) condition.

The highest CPSD levels are found at the BPF and the first few harmonics, with the strongest correlation occurring on the first two harmonics. In particular, the peak values are concentrated in the blade mid-span region ($0.5-0.9R$), suggesting that this portion of the blade contributes most significantly to the generation of tonal noise. This behaviour is consistent with the increase in blade loading and local rotational velocity toward the outer blade sections.
Moving toward the hub ($x/R < 0.3$), the correlation levels decrease, indicating a weaker acoustic contribution from the inner part of the blade, where the circumferential velocity and aerodynamic loading are lower. Similarly, beyond the blade tip, thus outside the rotor disk ($x/R > 1$), the CPSD rapidly decreases across all harmonics. Higher-order harmonics remain visible up to approximately the tenth BPF harmonic, although their amplitude gradually decreases with increasing frequency. The persistence of these harmonics suggests that the acoustic emission is primarily governed by periodic blade-flow interactions associated with propeller rotation.
Fig. 7 b) shows the CPSD distribution obtained for the two-bladed APC 5.25×4.75 propeller. The comparison with the toroidal geometry indicates that the aeroacoustic sources of both propellers remain concentrated in the outer blade region; however, the toroidal geometry appears to reduce the coherence between local flow fluctuations and radiated sound, particularly near the tip region and at higher frequencies. These results support the hypothesis that the toroidal blade-tip design mitigates some of the noise-generating mechanisms typically associated with conventional open-tip propellers.

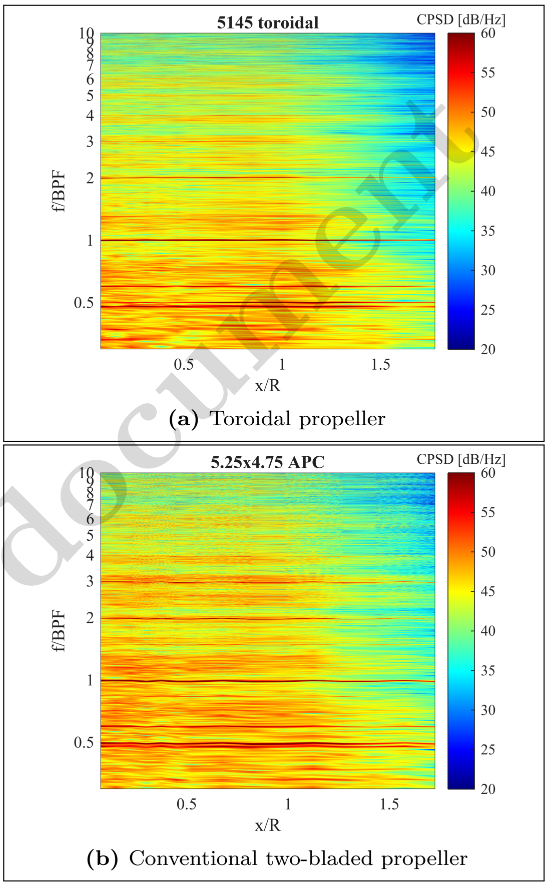

(a) Toroidal propeller

(b) Conventional two-bladed propeller

Figure 8: CPSD between the local velocity fluctuations measured at different radial positions and the far-field acoustic pressure signal from the furthest observer position. With incoming flow at 20 m/s.

The introduction of a 20 m/s crossflow (Fig. 8) increases the velocity-pressure coherence for both propellers and shifts the correlated structures downstream, consistent with the displacement of the wake observed in the flow-field measurements. The results suggest that, under forward-flight conditions, inflow-induced loading fluctuations become an increasingly important noise-generation mechanism, reducing the relative influence of blade-tip effects that dominate the hover case. Consequently, the aeroacoustic differences between toroidal and conventional geometries appear less pronounced than in static conditions, although the toroidal propeller still exhibits evidence of a weaker concentration of coherent tip-related noise sources.

4. Conclusion

This work presented an experimental investigation of the aerodynamic and aeroacoustic performance of nine commercially available 5-inch UAV propellers, including conventional two-bladed and three-bladed configurations, a winglet-equipped design, and a toroidal propeller.

Under hover conditions, all propellers exhibited similar wake velocity distributions, characterized by a velocity minimum at the hub, a maximum in the intermediate span region, and a gradual decay outside the rotor disk. The relative turbulence level reached its highest values near the blade tip region, suggesting the importance of tip-related flow structures.

The acoustic measurements revealed a clear influence of blade count and geometry on noise generation. Conventional two-bladed propellers generally produced higher OASPL levels than three-bladed configurations. Among the latter, propellers with larger pitch angles and larger diameter exhibited the lowest noise emissions.

The toroidal propeller consistently showed lower noise levels than the conventional two-bladed propellers while maintaining acoustic emissions comparable to several three-bladed configurations. These results confirm the potential of toroidal blade-tip geometries as an effective passive noise-mitigation strategy.

Spectral analysis highlighted significant differences in the broadband component of the acoustic emissions. The APC 5×5E generated the highest low- and mid-frequency noise levels, whereas the T5143S exhibited among the largest contributions at high frequencies. The GF 5152S-3, characterized by the highest pitch angle, showed the lowest high-frequency broadband noise.

The introduction of a 20 m/s incoming flow substantially modified both the aerodynamic and acoustic fields. The wake was displaced downstream and the measured OASPL increased by approximately 4-8 dB for all propellers. Under these conditions, the toroidal propeller became the quietest configuration, while conventional two-bladed propellers remained among the noisiest.

CPSD analysis demonstrated that tonal noise generation is primarily associated with velocity fluctuations occurring in the outer blade region, approximately between $0.5R - 0.9R$. For the conventional propeller, elevated coherence persisted closer to the blade tip, whereas the toroidal geometry exhibited lower coherence levels and a more diffuse spatial distribution, indicating a mitigation of tip-related noise-generation mechanisms.

Overall, the results indicate that blade-tip geometry has a significant impact on the aeroacoustic behaviour of small UAV propellers. While conventional blade design parameters such as pitch angle, diameter, and blade count influence both tonal and broadband noise generation, the toroidal geometry appears particularly effective in reducing wake-related aeroacoustic sources, especially under forward-flight conditions. These findings suggest that toroidal propellers represent a promising solution for the development of quieter UAV platforms, although further work is required to assess their performance under matched-thrust operating conditions and during realistic flight manoeuvres.

References

[1] J. Sun, K. Yonezawa, Y. Tanabe, H. Sugawara, and H. Liu, “Blade twist effects on aerodynamic performance and noise reduction in a multirotor propeller,” *Drones*, 2023. DOI: 10.3390/drones7040252.

[2] R. Noda, M. Hirose, T. Nakata, and H. Liu, “Low-noise propeller design with enlarged blade area for drones,” *J. Robotics Mechatronics*, vol. 37, pp. 799–806, 2025. DOI: 10.20965/jrm.2025.p0799.

[3] T. Zhang, Z. Cheng, C. Zhao, Y. Wang, Y. Zhao, and Y. Liu, “Noise reduction mechanism of a bio-inspired rotor blade with forward–backward swept tip,” *Physics of Fluids*, 2026. DOI: 10.1063/5.0318862.

[4] J. Rong et al., “Owl-inspired leading-edge serrations for aerodynamic noise mitigation in drone propellers,” *Physics of Fluids*, 2025. DOI: 10.1063/5.0268150.

[5] Y. Wei et al., “Experimental investigation of a biomimetic propeller coupled with owl-inspired leading and trailing edges serrations,” *Physics of Fluids*, 2025. DOI: 10.1063/5.0266266.

[6] W. Wei, Y. Ma, S. Wei, D. Wang, M. Guo, and Q. Yan, “Analysis and evaluation of aerodynamic noise characteristics of toroidal propeller,” *Drones*, 2024. DOI: 10.3390/drones8120753.

[7] M. Shekh and S. Rani, “Optimization of UAV propeller performance through design, development, and testing of diverse propeller geometries,” *Proceedings of the Institution of Mechanical Engineers, Part G: Journal of Aerospace Engineering*, vol. 240, pp. 1020–1043, 2025. DOI: 10.1177/09544100251400497.

[8] J. Sun, K. Yonezawa, E. Shima, and H. Liu, “Experimental investigations on aerodynamic and psychoacoustic characteristics of three-blade looprop propeller,” *The Journal of the Acoustical Society of America*, 2023. DOI: 10.1121/10.0023064.

[9] P. Li, C. Liu, Y. Liu, and Y. Yang, “Multi-objective design and evaluation of a toroidal rotor for quadcopters,” *Physics of Fluids*, 2024. DOI: 10.1063/5.0243175.

[10] M. Chen, T. Liu, J. Edwards, and T. Fang, “Computational study of hybrid propeller configurations,” *Aerospace*, 2026. DOI: 10.3390/aerospace13010094.